IEEE Access
Multidisciplinary | Rapid Review | Open Access Journal

Received April 16, 2021, accepted April 26, 2021, date of publication April 29, 2021, date of current version June 4, 2021.

Digital Object Identifier 10.1109/ACCESS.2021.3076507

Metal Surface Guided-Wireless Power Transfer System for Portable Applications With Multiple Receivers

FRANKLIN BIEN, (Senior Member, IEEE), WOOJIN PARK, (Graduate Student Member, IEEE), BONYOUNG LEE, (Graduate Student Member, IEEE), AND GANGIL BYUN, (Member, IEEE)

Department of Electrical Engineering, Ulsan National Institute of Science and Technology, Ulsan 44919, South Korea

Corresponding author: Franklin Bien (bien@unist.ac.kr)

This work was supported in part by Korea Electric Power Corporation under Grant R20XO02-20, and in part by the Basic Science Research Program of the National Research Foundation of Korea (NRF) funded by the Ministry of Science and ICT (MIST) under Grant NRF-2017R1A5A1015596.

ABSTRACT Recently, research has been actively conducted to overcome various challenges observed in wireless power transfer (WPT) technology. However, as additional techniques are implemented, the complexity and cost of WPT systems increased. Therefore, there is a need for a new WPT method that can overcome the shortcomings of existing technology. This paper presents a metal surface guided-wireless power transfer (MSG-WPT) system for applications with multiple receivers (Rxs). First, a plate-wire propagation enhancer (PWPE) is shown to improve the power transfer efficiency (PTE). However, it is not suitable for portable receiving systems. Based on our analysis of the PWPE characteristics, applying an L-section lumped impedance-matching scheme instead of a PWPE can improve the portability of the Rx. A coil-based propagation enhancer (CPE), or a coil-based inductor (CI), can increase the power received if it replaces the lumped inductor in the L-section scheme. The MSG-WPT system does not experience the co-alignment issues that exist between a pair of transceivers (TRxs) in conventional WPT systems. It can also support multiple Rxs while ensuring that the PTE of each Rx is relatively unaffected. An electromagnetic simulation of the proposed MSG-WPT system is performed using a high-frequency structure simulator (HFSS), and measurements are conducted in a corresponding experimental environment. The system power efficiency is measured at −12 dB in the 4 MHz frequency band. The proposed MSG-WPT system with a CPE is adequately efficient and portable, while also allowing a more liberal arrangement of Rxs compared to other conventional WPT systems.

INDEX TERMS Coil-based propagation enhancer (CPE), L-section lumped impedance matching, metal surface guided (MSG), plate-wire propagation enhancer (PWPE), wireless power transfer (WPT).

I. INTRODUCTION

Wireless power transfer (WPT) will change the way we use technology in the near future because it allows electronic devices to overcome the limitations of wired charging. Compared to a traditional wired system, WPT includes the convenience of not having to plug/unplug a device that needs to be charged and of the removal of multiple freely hanging wires, thereby adding an aesthetic benefit as well. Many smartphone users have been charging their phones via WPT instead of short-wired lines. Specifically, as wireless technology has evolved from 3G to LTE, and now to 5G, the faster data rates and processing speeds are causing phone batteries to drain faster. However, the limited energy density that each phone battery can handle within a certain size has prompted a search for ways to more frequently and conveniently charge the device. This inconvenience has led to a desire to charge conveniently regardless of the location and/or the orientation of the electronic device. Moreover, a considerable number of low-power Internet of Things (IoT) devices will prevail soon,

The associate editor coordinating the review of this manuscript and approving it for publication was Sun Junwei.

requiring each device to have a mean to be powered when the initially installed battery is discharged. If the IoT devices are configured with wired chargers, it may not have a power issue at the cost of complexity during installations. If the IoT devices are battery operated, replacing so many devices will cause maintenance issue. WPT allows a these IoT devices to become flexible, eliminating all such problems with no strings attached.

Electrically, WPT can be classified into two methods: radiative and nonradiative WPT. The former applies the far field of an electromagnetic (EM) wave for long-distance WPT, and the latter applies the near field of the EM wave for short- or intermediate-distance WPT. However, the far-field method has limited application due to issues with its safety and power transfer efficiency (PTE).

Among the near-field methods, inductive power transfer is now available commercially, with the Qi standard [1]. Research on magnetically coupled resonance (MCR)-WPT has been actively conducted since its publication in 2007 [2]. Recently, published work that proposes a WPT with a wider range and multiple Rx capabilities is mostly based on magnetically coupled resonance-wireless power transfer (MCR-WPT) because of its mid-range power transfer capability.

Many systems with MCR-WPT-based transceivers (TRxs) have been reported to enhance the PTE. Additionally, intermediate resonant coils have been presented based on a system analysis for improving the PTE [3]. For example, multi-transmitter (Tx) and array systems have been proposed to solve the misalignment problem [4]. Mode-reconfigurable resonators, which are capable of adaptively changing their resonant capacitances, have previously been proposed to address the sensitivity to alignment issue between TRxs [5]. To address the variable driving and loading configurations, special control circuits capable of adaptive switching according to the distance and misalignment situation have been developed [6]–[8]. To enhance the WPT range, array systems without auxiliary control circuits were proposed in [9]–[11]. For multiple Rxs, the application of resonant frequencies under specific load conditions was proposed in [12]. Furthermore, a method of cascading converters at the Rx was presented to modulate the equivalent load resistances for power distribution [13]. Additionally, an analysis of the optimal loads has been proposed to achieve the maximum efficiency in a typical single Tx and multi-Rx system [14]. In contrast with the single resonant frequency of the receiver, different resonant frequencies of the Rxs are applied in the MCR-WPT system [15]. These types of coil-based WPTs exhibit high PTE sensitivity depending on the degree of misalignment and the distance between TRxs. This is one of the major limiting factor for the MCR-WPT to prevail in consumer electronics. Therefore, a less stringent WPT system that can provide power to devices are required.

Metal surface guided (MSG) field propagation is a good candidate for a liberal WPT charging system. An MSG-WPT system provides a true 2-dimensional 'surface' as a charging plane. For example, imagine any table or desk that has aluminum foil installed underneath the surface. The whole table surface can be used as a charging spot, regardless of its orientation, its distance from the Tx, and the number of devices being charged. Recently, public charging spots based on inductive power transfer (IPT) WPT, such as Qi wireless charging standards, have been installed on tables in many fast-food restaurants and coffee shops for their convenience and aesthetics. Installations of these IPT based WPT system continues to increase around the world. However, these IPT-based charging systems can charge only one device at a time. Moreover, charging occurs only when the device is located exactly on top of the charging spot. This forms a single 'line' from the outlet to the charger.

In an MSG-WPT system, TRxs can be freely placed anywhere on the metal surface and remain coupled with each other. More importantly, the metal surface need not be exposed as the TRx can be coupled to the metal surface from a few mm apart. As a result, the metal surface can be covered for aesthetic purposes. Once of the most important benefit with MSG-WPT system is that wireless power transfer can be performed even when the TRxs are not aligned and when they are arranged on opposite sides of a thick metal wall [16]. This result is a remarkable advantage when considering the previously mentioned limitations of the MCR-WPT system.

From an economic point of view, relatively low-cost metal materials, such as aluminum foil, can be used without performance degradation. The proposed system consists of relatively simple TRxs and metal surfaces, such as aluminum foil or metal plates. As seen from references [3]–[15] in regard to MCR-WPT, overcoming the alignment issue and increasing the distance between TRxs while being capable of using multiple Rxs is quite challenging and requires a heavy and complex system. However, the MSG-WPT system does not face the abovementioned limitations that the MCR-WPT method overcomes with increased system complexity.

In this paper, we propose a metal surface guided-wireless power transfer (MSG-WPT) system and use a coil-based propagation enhancer (CPE) at the Rx to increase the received power and improve portability. We analyze and seek the tunable design parameters of the additional wire and metal plate, which is named the plate–wire propagation enhancer (PWPE). The analysis proves that the PWPE plays a crucial role in producing resonance and enhancing the PTE and that the plate and wire have capacitive and inductive characteristics, respectively. The PWPE affects both the PTE and the resonance frequency. Based on this fact, we substitute the PWPE at the Rx with a lumped inductor and capacitor. This substitution is considered an L-section impedance matching scheme, and from this, we derive the circuit model of the entire system. The substitution is found to increase the portability of the MSG-WPT system. To increase the received power, a coil-based inductor (CI) is employed in the L-section impedance-matching scheme instead of the lumped inductor. The magnetic field is distributed horizontally on the metal surface, where it couples with the CI. In summary, the CI plays two roles: it acts as a substitute for the lumped inductor

and provides additional magnetic field coupling on behalf of the Tx. Thus, the CPE increases the intensity of the received power while working as the inductor for impedance matching.

The remainder of this paper is organized as follows. An analysis of the PWPE and the proposed MSG-WPT system with the CPE are introduced in Section II. An equivalent circuit model of the MSG-WPT system and multiple-Rx MSG-WPT system are described in Section III, and the conclusions are presented in Section IV.

II. PROPOSED METAL SURFACE GUIDED-WIRELESS POWER TRANSFER SYSTEM

In this section, we present an analysis of the characteristics of the PWPE used in the receiving part of the previous research [16]. This analysis establishes that the excited EM field is guided on the metal surface and enhanced by the PWPE. Design factors from this analysis are reflected in our proposed MSG-WPT system. The PWPE is substituted with the CPE in the receiving part to improve the portability and enhance the power transfer of the proposed MSG-WPT system. We propose an MSG-WPT Rx with a CPE to improve the intensity of received power while allowing the MSG-WPT system to be more compact and portable by eliminating the PWPE for its practical application in the future.

A. ANALYSIS OF PLATE-WIRE PROPAGATION ENHANCER

In the proposed MSG-WPT system, when the EM field propagates on the metal surface, the H-field is perpendicular to the propagation direction as the E-field is perpendicular to the metal surface. Hence, the proposed MSG-WPT system propagates in transverse magnetic (TM) mode. Moreover, through the E-field and H-field equations, it can be seen that the intensity of the EM field in the direction perpendicular to the metal surface attenuates evanescently.

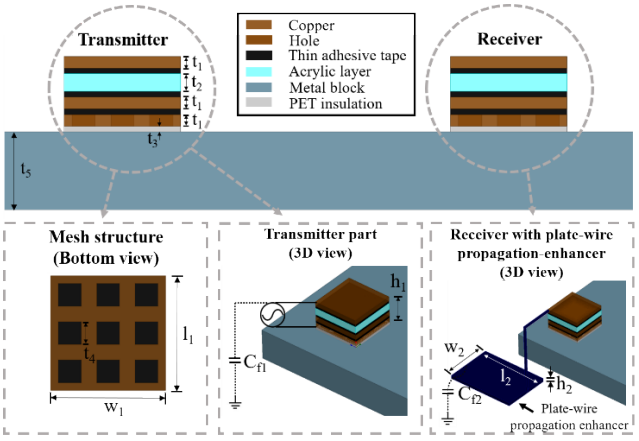

FIGURE 1. Standalone TRx structure and connection with the plate-wire propagation enhancer (PWPE).

MSG field propagation on a metal surface has been previously reported for WPT over a metal wall [16]. The transmitting and receiving structure is designed with a mesh-based copper plate and several dielectric layers, as shown in Fig. 1. Mesh-based copper plate TRxs play the role of a planar ground-backed impedance (GBI) surface [17], establishing a TM wave throughout the metal surface due to the inductive sheet [18]. The TRxs have an extremely low profile in which the length of the square of the TRx is $0.002\lambda_0$(150 mm), where λ_0 is the wavelength of the resonance frequency (4 MHz). Details of the length of the TRx and other parameters of the system are shown in Table 1.

TABLE 1. Parameters of the TRx and PWPE Architecture.

Parameter	Value (mm)	Parameter	Value (mm)
t_1	1	t_2	1.5
t_3	1	t_4	30
t_5	1	w_1	150
w_2	300	l_1	150
l_2	400	h_1	4.5
h_2	1		

We conducted tests over five different kinds of metal materials for the MSG-WPT system: stainless steel plates, copper plates, aluminum plates, aluminum foil and steel plates. All experiments were performed in the same experimental environment and under the same experimental conditions, such as the size of the metal plate, distance between two TRxs, and input power intensity. The experimental configuration was carried out by generating specific power from the Tx side while measuring the received power intensity with the spectrum analyzer connected to the Rx. According to the results of the experiments, the received power intensity is measured to have a less than 1 dB difference depending on the type of metal plate. This result means that the MSG-WPT system can be used over a wide range of metal materials with similar performance. In addition, the thickness of the metal material is also found to have little effect on the efficiency of the MSG-WPT system, as shown in the case of the aluminum foil and plate. According to the conductivity table, the conductivity of stainless steel is approximately 1.4e6 S/m, copper is approximately 5.96e7 S/m, aluminum is approximately 3.5e7 S/m, and steel is approximately 1e6 S/m; thus, all have high electrical conductivity. The greater the electrical conductivity is, the closer the properties of the metal are to being the perfect electrical conductor (PEC), which is an idealized material that exhibits infinite electrical conductivity and would provide an environment in which MSG-WPT can perform better. Based on an earlier investigation, most metals have high electrical conductivity, so the MSG-WPT system can be built using any metal material at the designed frequency. Therefore, aluminum foil is chosen as the metallic path for the MSG-WPT system because aluminum foil is reasonably priced, convenient to install/uninstall during experiments, and easy to purchase at any marketplace.

An additional metal plate is added at the Rx to reinforce the PTE, as shown by the third gray-dashed box in Fig. 1. However, the previous system [16] has a critical disadvantage for practical use in wireless power transfer areas due to the separate free-hanging PWPE outside the Rx. Although the

system using [16] can have simplified components composed of a Tx and an Rx with a PWPE attached, it is not suitable for portable devices or systems because of the explicit requirement of the PWPE to be touching a physical ground. Thus, for [16] to be used in practical applications, the PWPE needs to be replaced by a more compact and portable form.

To substitute the PWPE, we conducted a detailed analysis of the PWPE to understand how the PWPE plays a critical role in MSG-WPT, which is missing from [16]. Structurally speaking, MSG-WPT with a PWPE is observed with two major variable factors. The first component is the length of the wire between the Rx and PWPE, and the second component is the size of the metal plate composing the PWPE. As the length of the wire increases, the inductance value increases between the Rx and PWPE in series. Similarly, a PWPE with a larger metal plate has an increased capacitance value. Hence, the length of the wire and the size of the metal plate affect the resonance frequency of the MSG-WPT system. Based on the resonance frequency equation we assume that the resonance frequency of the MSG-WPT system can also be affected by the wire length and the plate size of the PWPE.

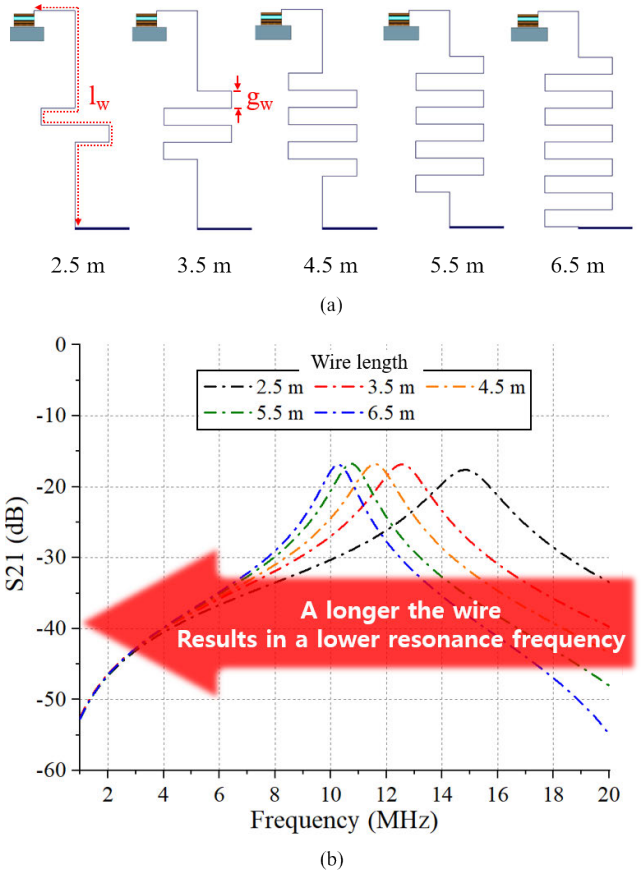

FIGURE 2. Simulation setup environment and the results with respect to the wire length of the PWPE: (a) Side view of the Rx with the PWPE for wire lengths from 2.5 to 6.5 m. (b) Tx-to-Rx voltage gain (S_{21} parameter) results with various wire lengths.

Fig. 2 shows the simulation test setup and the results of the design parameter of the PWPE: inductance. Fig. 2 (a) shows the side view of the extension of the wire (l_w) of the PWPE. The distance between the metal plate of the PWPE and the metal block is fixed, and the wire gap (g_w) is large enough to prevent the effects of additional parasitic capacitance. A distance of 1.5 m is set between the top layer of the Rx and the PWPE to minimize the effect of g_w and highlight the effect of l_w. Fig. 2 (b) shows the variation in S_{21} when the length of l_w is increased from 2.5 to 6.5 m, where the increase in inductance negatively affects the resonance frequency. On average, an increase of approximately 8.6% in the resonance wavelength is observed for every meter increase in l_w. The effective resonance wavelength, without the PWPE, is approximately 14.7 m. When the resonance frequency is 11.5 MHz ($l_w = 4.5$ m), the dominance of the PWPE in the MSG-WPT system is approximately 23% = (4.5 m / (4.5 m + 14.7 m)), in terms of the wavelength composition ratio. We concluded that the PWPE components heavily affect the resonance frequency and the PTE. Based on this analysis, we present the proposed portable MSG-WPT system in Section II. B.

Fig. 3 illustrates the electric field distributions of the two cases: the Rx with and without the PWPE. Fig. 3 (a) shows the test setup and simulation results of the high-frequency structure simulator (HFSS). The Tx and Rx are placed on the metal surface, and the distance between two TRxs is approximately 1.5 m. The brown rhombuses are the TRxs, and the blue quadrangle is the metal structure. The navy rhombus with a thin wire attached to the Rx is the PWPE, as shown in Fig. 1. Fig. 3 (b) shows the electric field distributions of the two cases. The measurement plane is the side of the Rx, as shown on the x-z plane in Fig. 3 (a), where 3pf is added to reflect the fringing capacitance C_f between the Tx and the earth ground. As shown, a larger electric field can compactly exist on the metal surface when the PWPE is used. The E-field distribution at the higher position in the system with the PWPE shows a lower intensity, which means less radiation. On the other hand, the E-field distribution at the lower position in the system with the PWPE shows a higher intensity. This result means that the Rx with the PWPE can pick up more power from the metal surface. Details of the magnitude of the electric field distribution are shown in Fig. 3 (c).

B. PROPOSED SYSTEM WITH THE COIL-BASED PROPAGATION ENHANCER

In this section, we present a method to substitute the PWPE and propose the optimal form of the Rx for the MSG-WPT system. We have shown that the PWPE definitely contributes to MSG propagation. The MSG-WPT system is completed with additional inductive and capacitive components on the Rx in terms of the PTE and resonance. On the other hand, the PWPE has a relatively long wire and wide plate, which makes the Rx quite bulky. Therefore, we decided to substitute the PWPE with an inductor and capacitor to enhance its portability. Based on the analysis of the PWPE, the Rx with the PWPE in the MSG-WPT system can be

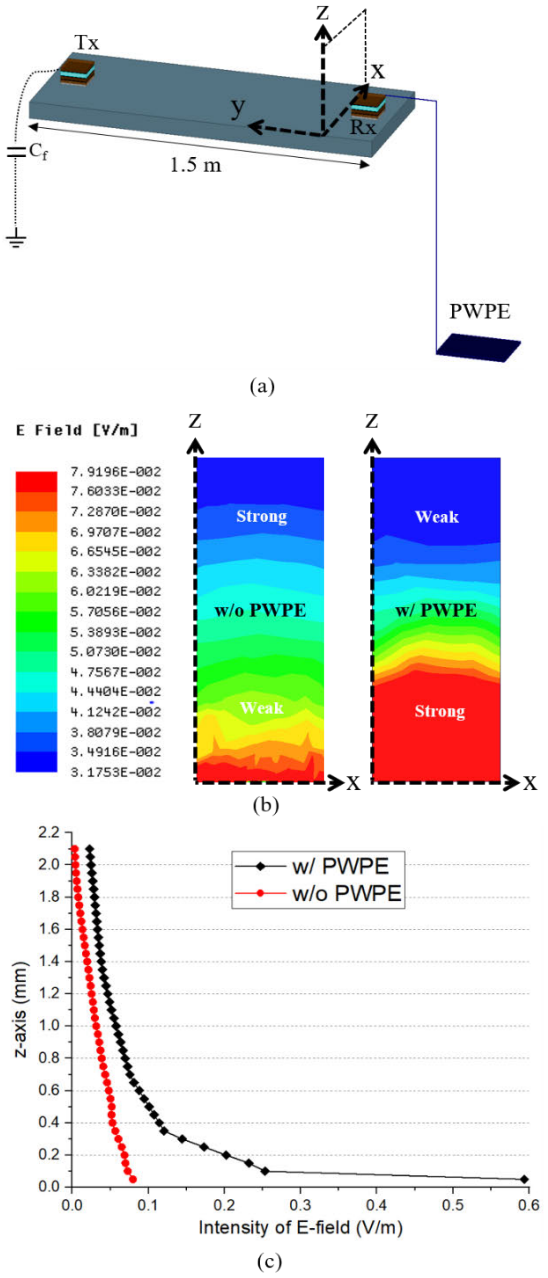

FIGURE 3. Difference in the level of the electric field from the metal surface to air, with and without the PWPE. (a) Simulation test setup. (b) Electric field distribution on the metal surface. (c) Detailed magnitude of the electric field distributions in each case.

represented with additional inductive and capacitive components in terms of the resonance. In Fig. 4, without the PWPE, 50-ohm impedance matching of the L-section structure using a lumped inductor and capacitor is applied at the targeted resonance frequency of 4 MHz. The detailed parameters of the matching circuit are displayed in Table 2.

Fig. 5 (a) illustrates the voltage reflection coefficient (S_{11} parameter) of the MSG-WPT Rx, with and without the lumped impedance-matching scheme. The measurement was performed with a E5061B ENA Series network analyzer

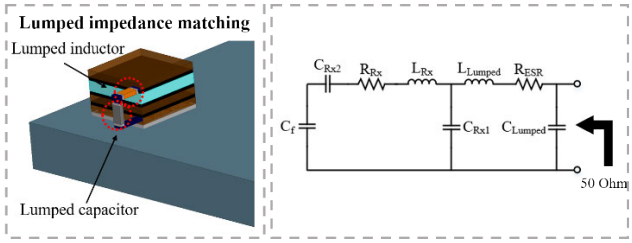

FIGURE 4. L-section 50 Ω lumped impedance-matching scheme for the Rx with the lumped elements substituting the PWPE.

TABLE 2. Parameters of the RX and the matching scheme.

Parameter	Value	Parameter	Value
R_{Rx}	12.1	X_{Rx}	−172.2
L_{Lumped}	7.69 μH	C_{Lumped}	1.4 nF

made by Keysight Technologies. The Rx without any kind of propagation enhancer (PE), such as the PWPE, lumped impedance matching, and CPE, does not show characteristics as an antenna because there is no range of S11 peaks (generally less than −10 dB). On the other hand, approximately −28 dB is observed with lumped impedance matching, showing the targeted resonance feature.

Fig. 5 (b) illustrates the Smith charts for the two cases. The center of the circle represents 50 Ω, and the impedance of the Rx must be positioned at that point. As shown, before the addition of the lumped impedance-matching circuit, the imaginary value of the impedance dominated the real value. The 50 Ω impedance of the Rx is achieved at 4 MHz after adding the lumped impedance matching, as depicted by the solid line. In addition, the TRxs are identical, except for the PE, and present the same impedance characteristics.

Fig. 5 (c) shows the results of the received power with a single tone at 4 MHz, measured on an Agilent PXA N9030A signal analyzer. As in the lumped impedance-matching case, both the Tx and Rx are applied. The red line represents the received power with lumped impedance matching, and the black line represents the received power without lumped impedance matching. The transmitting power is 30 dBm (1 W), and each received power intensity is approximately 6 dBm (4 mW) and 14 dBm (25 mW). That is, the system with lumped impedance matching has 8 dB (6.3 times) greater efficiency than the system without lumped impedance matching. Therefore, we confirm that the PE still works for the MSG-WPT system with lumped elements.

When the MSG field is excited on a metal surface, an E-field is formed perpendicular to the metal surface, and an H-field is formed horizontally. As a result, an H-field can be received using a coil-based inductor (CI) to improve the received power intensity. To demonstrate the effect of the CI, an MSG-WPT Tx is placed on the metal surface, while a CI with a resistive load is placed on the metal surface 1.5 m away with various geometrical orientations. The test results are shown in Fig. 6. A 50 Ω resistor is applied to the coil inductor as a load and placed on the metal surface to receive

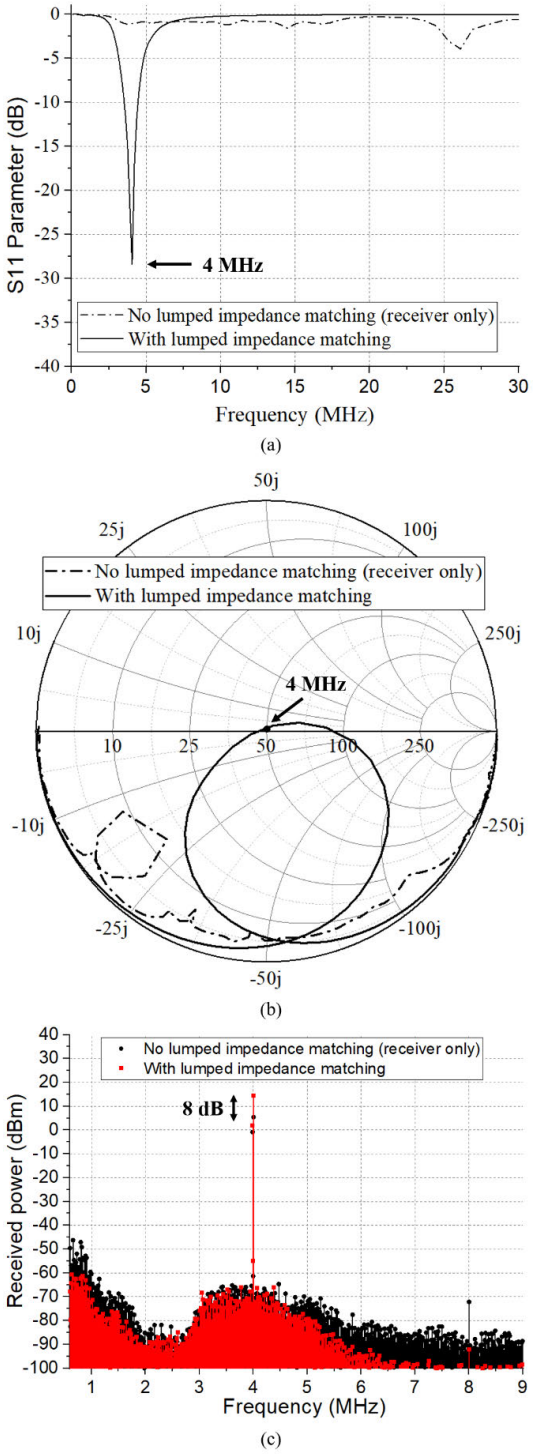

FIGURE 5. Measured system characteristics of the two cases: no lumped impedance matching (TRx only) and lumped impedance matching. (a) Voltage reflection coefficient (S_{11} parameter). (b) Smith chart characteristics. (c) Received power level with a single tone at 4 MHz obtained on the signal analyzer.

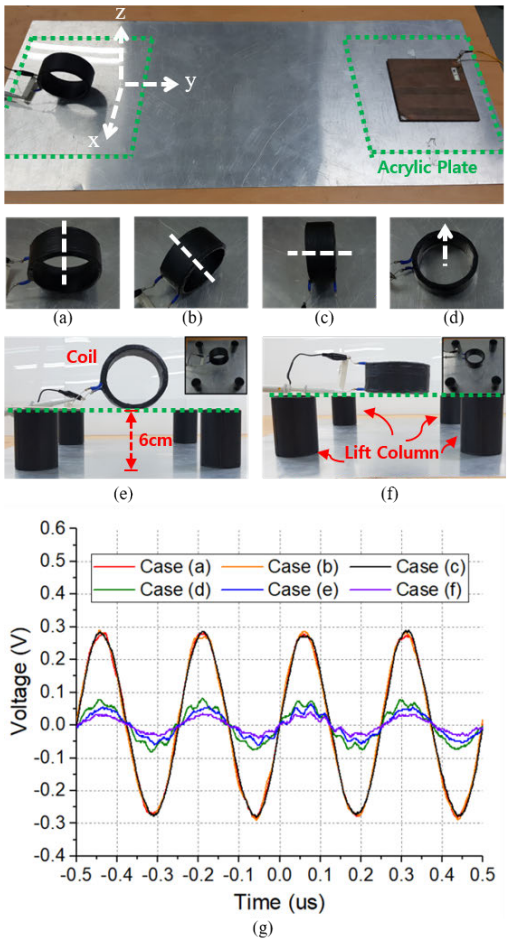

FIGURE 6. Photographs of the test setup and the measured voltage results of the CI for various geometrical orientations on the metal surface or 6-cm away from the metal surface: (a) CI axis parallel to the x-axis of the metal surface. (b) CI axis aligned at 45 degrees to the x-y plane on the metal surface. (c) CI axis parallel to the y-axis of the metal surface. (d) CI axis parallel to the z-axis of the metal surface. (e) CI axis parallel to the x-axis and 6 cm away from the metal surface. (f) CI axis parallel to the z-axis and 6 cm away from the metal surface. (g) Measured waveform of the voltage at the resistive load of the CI.

the MSG field. The specific parameters of the CI are shown in Table 3.

Fig. 6 displays six different orientations and/or distances of the CI and the corresponding measured voltages. The 1 W input power is supplied with a single tone at 4 MHz to the Tx. A higher voltage is induced in the CI when the CI axis is parallel to the x-y axis on the metal surface, as shown in Fig. 6 (a), (b), and (c). In Fig. 6 (a) and (c), a significant angle difference of 90° causes only a 3% difference between the measured voltages. Therefore, we conclude that the orientation of the CI axis on the x-y plane is free once the CI axis is parallel to the metal surface. Additionally, coaxial alignment-free features between the TRxs can be observed even with this CI. In Fig. 6 (d), the CI axis is normal to the metal surface, receiving 32–35% lower voltage, which can be attributed to the higher magnetic flux linkage associated with the parallel CI axis. Fig. 6 (e) and (f) show the CI aligned as in Fig. 6 (a) and (d), respectively, but placed 6 cm above the metal surface, to investigate the exponential decay of the field strength when away from the metal–air interface. The specific values of the voltage in each case are presented

in Fig. 6 (g). This test is performed with a Keysight Infinivision MSOX3034T mixed signal oscilloscope.

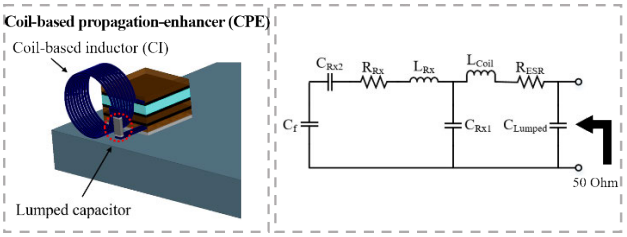

FIGURE 7. L-section 50 Ω impedance-matching scheme using the CI instead of the lumped inductor for the optimal receiving part of the MSG-WPT system.

Based on the CI experiments, we employ the CI instead of the lumped inductor to improve the received power intensity, which enhances the field absorption at the receiving part, as shown in Fig. 7. The center axis of the CI is parallel to the metal block to pick up the MSG magnetic field that exists on the metal surface. The detailed parameters of the CI are presented in Table 3.

TABLE 3. Parameters of the coil-based structure.

Radius (mm)	Wire thickness (mm)	Inductance (μH)	Rs (Ω)	Turns (#)
40	2	7.65	0.72	9

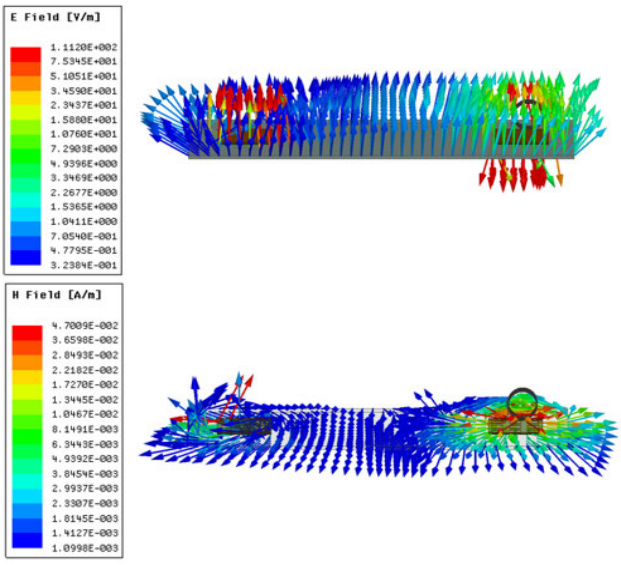

FIGURE 8. Electric- and magnetic-field distributions of the MSG-WPT with the CPE, as obtained from the HFSS simulations.

Fig. 8 illustrates the electric and magnetic-field distributions of the MSG-WPT with the CPE obtained from the HFSS simulations. The organization of the Rx with the CPE is shown in Fig. 4. The electric field is normal to the metal surface, and the magnetic field is parallel to the metal surface. As demonstrated in Fig. 6, the CI can pick up the parallelly aligned magnetic field on the metal surface and reinforce the received power level.

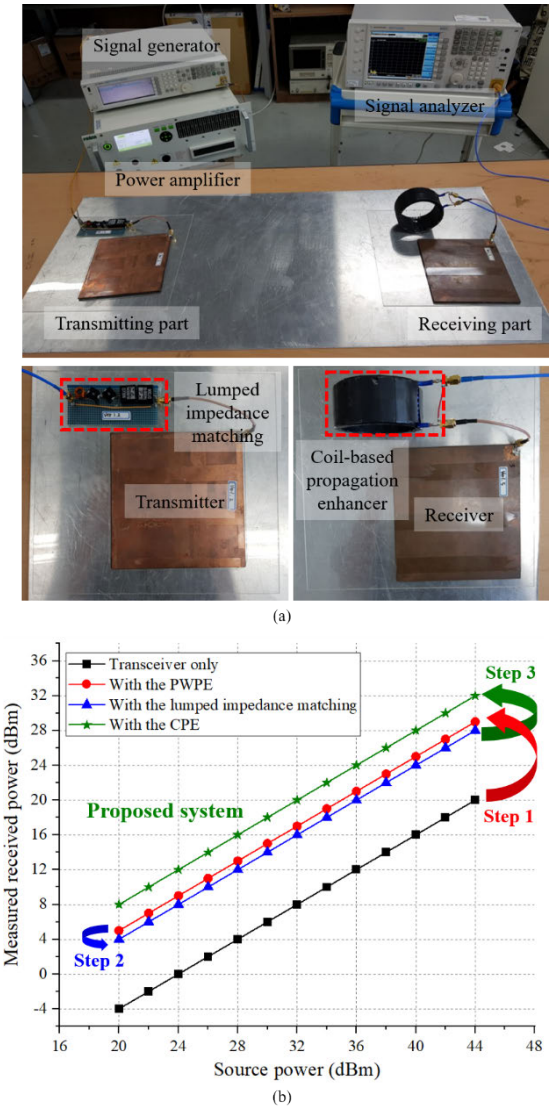

FIGURE 9. Photograph of the proposed MSG-WPT system with the CPE. (a) Test setup of the proposed MSG-WPT system with the CPE. (b) Measured received power intensity according to the source power level.

Fig. 9 shows the test setup environment and the results of the proposed MSG-WPT system with the CPE. As shown in Fig. 9 (a), the lumped impedance-matching circuit is applied to the Tx, and the CPE is applied to the Rx. The distance between the TRxs is 1.5 m. The source power comes from the signal generator and power amplifier at the Tx, and the signal analyzer measures the received power intensity at the Rx. Fig. 9 (b) shows the measured results of four cases: with only the TRx, with the PWPE, with lumped impedance matching, and with the CPE. The CPE case achieves the highest efficiency of approximately –12 dB. The PWPE and lumped matching cases exhibit similar efficiencies of

approximately −16 dB. The case of only the TRx exhibits the worst efficiency of approximately −24 dB.

III. ANALYSYS OF THE PROPOSED MSG-WPT SYSTEM

In the following paragraphs, we present the equivalent-circuit model of the proposed MSG-WPT system with the PWPE and the CPE. The comparison of the S_{21} parameters from the two different simulation tools, Cadence and HFSS, is also presented. Moreover, experiments using MSG-WPT with a system of multiple receivers are presented.

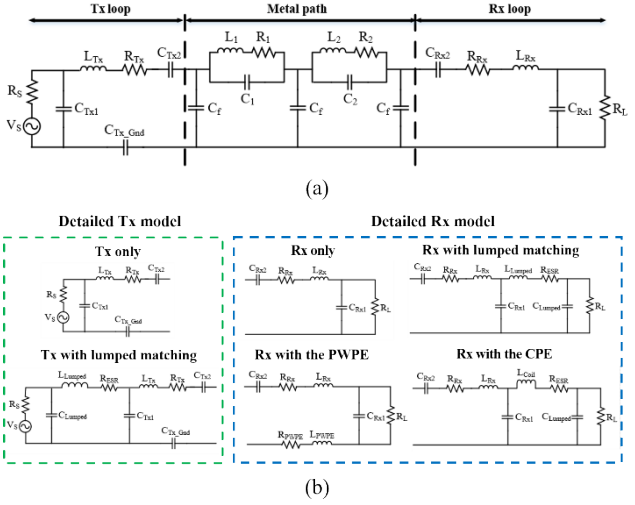

FIGURE 10. Equivalent circuit model of the MSG-WPT system: (a) General case including the Tx, metal path and Rx; (b) Elaborated Tx and Rx equivalent circuit models with lumped matching, the PWPE and the CPE.

A. EQUIVALENT CIRCUIT OF THE PROPOSED SYSTEM

Fig. 10 shows the equivalent-circuit model of the proposed MSG-WPT system. The basic equivalent-circuit model of the MSG-WPT system is shown in Fig. 10 (a). It consists of three parts: a Tx loop, metal path, and Rx loop. The power source, the resistance of the source, and the components (i.e., C_{TX}) of the Tx are in the Tx loop. The Rx loop contains the load resistance and the components (i.e., C_{RX}) of the Rx. The metal path can be expressed by an N-repetition of series inductances (i.e., L_1, L_2, …, L_N), resistances (i.e., R_1, R_2, …, R_N), and shunt capacitances (i.e., $C_1, C_2, \ldots, C_N$) per unit length. We find that the equivalent model is almost identical if N is greater than 4; therefore, we adopt $N = 4$.

Fig. 10 (b) shows the different variations of the Tx and Rx loops. There are two variations for the Tx loop and four variations for the Rx loop. The TRx can be simply represented by capacitors from the parallel copper layers and the series inductor from the GBI structure. In the lumped impedance-matching case, shunt capacitances and series inductances are added to the TRx, and the R_{ESR} is the equivalent series resistance of the inductance. The PWPE can be expressed as a single series inductance, R_{ESR}, and two capacitances. As shown in Fig. 1, the PWPE is composed of a single wire and a metal plate. The wire acts as the series inductance, and the plate makes two capacitances with the metal path and the building ground. The CPE is composed of the CI and the matching capacitance.

The simulated comparison of the S21 parameters obtained using two simulation tools is shown in Fig. 11, which shows that the equivalent circuit model is reliable in terms of the shape of S21 and the resonance frequency. The black solid line is from Cadence, which is one of the EDA tools for system circuit design. The black dashed line represents the simulation result from the HFSS. When the metal path is expressed as a circuit, it can be seen as a parallel structure with a dominant inductance and a relatively small value of capacitance, showing the effect of a band stop filter. Therefore, the S21 parameter value rapidly decreases at approximately 16 MHz and 50 MHz.

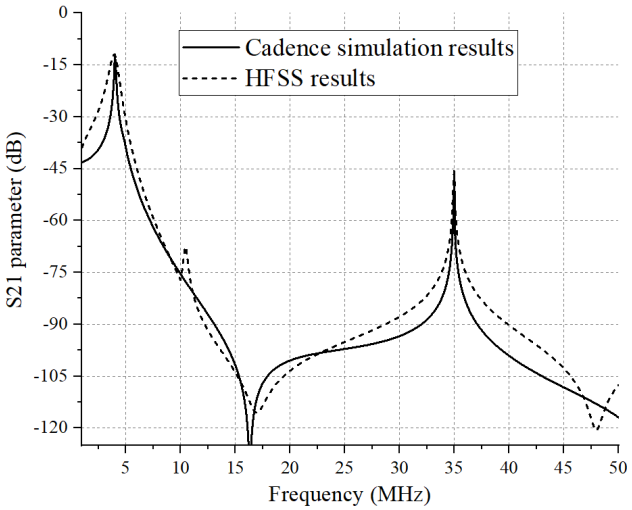

FIGURE 11. Comparison of the S_{21} parameters between the two simulation tools: Cadence and HFSS.

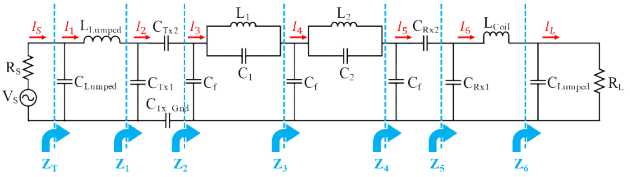

FIGURE 12. Simplified equivalent circuit of the MSG-WPT system including the IM and CPE at the TRx.

Fig. 12 shows a simplified equivalent circuit of the MSG-WPT system including the IM and CPE at the TRx to calculate the PTE of the entire MSG-WPT system. To simplify the calculation, components that do not significantly affect the PTE are neglected in the equivalent circuit. For numerical analysis, the equivalent circuit is first divided into multiple sections by unit components, as shown by the blue dotted line in Fig. 12. The impedance for each section (Z_1, Z_2,, Z_6) can be calculated, and the total PTE of the

MSG-WPT is derived by applying Kirchhoff's current law.

$$\begin{cases} I_1 = I_S \times \dfrac{Z_{C\_Lumped}}{Z_{C\_Lumped} + Z_{L\_Lumped} + Z_1} \\ I_2 = I_1 \times \dfrac{Z_{C_{Tx1}}}{Z_{C_{Tx1}} + Z_{C_{Tx2}} + Z_2 + Z_{C_{Tx_{Gnd}}}} \\ I_3 = I_2 \times \dfrac{Z_{C_f}}{Z_{C_f} + Z_{L1\|C1} + Z_3} \approx I_2 \\ I_4 = I_3 \times \dfrac{Z_{C_f}}{Z_{C_f} + Z_{L2\|C2} + Z_4} \approx I_3 \\ I_5 = I_4 \times \dfrac{Z_{C_f}}{Z_{C_f} + Z_{C_{Rx2}} + Z_5} \approx I_4 \\ I_6 = I_5 \times \dfrac{Z_{C_{Rx1}}}{Z_{C_{Rx1}} + Z_{L_{Coil}} + Z_6} \\ I_L = I_6 \times \dfrac{Z_{C\_Lumped}}{Z_{C\_Lumped} + R_L} \end{cases}$$

$$(Z_{C\_f} \gg Z_{L1\|C1}, Z_{L2\|C2}, Z_{C\_Rx2}, Z_3, Z_4, Z_5) \quad (1)$$

From (1), the load current can be expressed by the formula of the source current.

$$\begin{aligned} I_L = I_S \times & \frac{Z_{C\_Lumped}}{Z_{C\_Lumped} + Z_{L\_Lumped} + Z_1} \\ & \times \frac{Z_{C\_Tx1}}{Z_{C\_Tx1} + Z_{C\_Tx2} + Z_2 + Z_{C\_Tx\_Gnd}} \\ & \times \frac{Z_{C\_Rx1}}{Z_{C\_Rx1} + Z_{L\_Coil} + Z_6} \times \frac{Z_{C\_Lumped}}{Z_{C\_Lumped} + R_L} \end{aligned} \quad (2)$$

Once the impedance of each section and the related current are obtained, the PTE of the MSG-WPT system can be calculated. Additionally, the source and load impedance are assumed to be matched at 50 ohms, and the PTE can be expressed as (3), as shown at the bottom of the page.

To understand the critical components that affect the PTE of the MSG-WPT system, (3) can be utilized for improvements. As the physical size of TRx changes, the values of C_{TRx1} and C_{TRx2} also change accordingly. To match the changed C_{TRx1} to the 50-ohm impedance, the values of C_{Lumped}, L_{Lumped} and L_{Coil} must change accordingly, and these changes will affect the PTE. Finally, in the case of the metal path influence, as the value of C_f is relatively small, any leak through C_f is negligible, resulting in little effect on the PTE change of the MSG-WPT system.

B. MULTIPLE RXs OF THE MSG-WPT SYSTEM

It is true that the efficiency of a single Rx seems low at -12 dB (6.3%). However, when experimenting with multiple Rxs, each Rx receives the same amount of power. The received power efficiency is measured with a spectrum analyzer, while evenly transmitted power to multiple Rxs is visually illustrated with light bulbs that do not dim with additional Rxs on the same metal plate. Even if the number of Rxs is increased while the input power is maintained at a constant level, the power of the previously placed Rx does not decrease. Figs. 13 and 14 show the application of the MSG-WPT system in a multiple-receiving environment. Typical aluminum foil is laid on the table as the metal path of the multiple-receiving system, thereby showing the simplicity of establishing the system. Fig. 15 shows the measured voltage across the LED at the input of Rx #1 compared when the Rx is by itself and when four Rxs are lit.

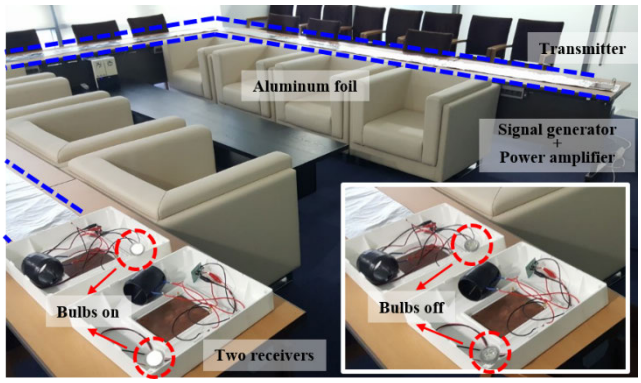

FIGURE 13. Test setup of the multiple-receiving MSG-WPT system with two Rxs using a 4 W bulb on 15 m of U-shaped aluminum foil.

In the case of Fig. 13, the aluminum foil is arranged in a U shape that follows the table setup. Two receivers with 4 W LED bulbs are placed on the aluminum foil 15 m away from the transmitter. When the power source (i.e., the signal generator and power amplifier) is on, each bulb turns on.

$$\begin{cases} P_{in} = I_S^2 R_s \\ P_{out} = I_L^2 R_L \\ PTE = \dfrac{P_{out}}{P_{in}} = \dfrac{I_L^2 R_L}{I_S^2 R_s} = \left(\dfrac{I_L}{I_S}\right)^2 \quad (\text{if } R_S = R_L) \\ = \left(\dfrac{Z_{C_{Lumped}}}{Z_{C_{Lumped}} + Z_{L_{Lumped}} + Z_1} \times \dfrac{Z_{C_{Tx1}}}{Z_{C_{Tx1}} + Z_{C_{Tx2}} + Z_2 + Z_{C_{Tx_{Gnd}}}} \right. \\ \left. \times \dfrac{Z_{C\_Rx1}}{Z_{C\_Rx1} + Z_{L\_Coil} + Z_6} \times \dfrac{Z_{C\_Lumped}}{Z_{C\_Lumped} + R_L} \right)^2 \end{cases} \quad (3)$$

To increase the number of Rxs, four sets of receivers equipped with 4 W LED bulbs are placed on aluminum foil, as shown in Fig. 14. The aluminum foil is approximately 3.5 m in length, and the Rxs are in a row from the opposite side of the Tx.

In these two tests, the operating frequency is 4 MHz, and the input power is set to 50 dBm (approximately 100 W), which is the minimum input power required to light up each bulb. The Tx with the power source excites the MSG field on the aluminum foil. The bulb shines brightly only when the Rx is placed right on the surface of the aluminum foil, which verifies that the power is transferred through the metal surface and not through air. There is no change in the state of the bulb, such as the bulb being turned off or a brightness change, when other Rxs are placed on the foil. This result means that the MSG-WPT system with multiple Rxs is applicable in situations that feature quasi-equivalent power transfer efficiency among the Rxs. Of course, if the number of Rxs to be placed increases beyond a certain number, the PTE of the system and the number of Rxs will not be proportional since the input power is limited. Due to the limited number of measurement equipment, we experimented with up to 4 Rxs in this environment. In conclusion, the MSG-WPT system is suitable for application in environments with multiple Rxs.

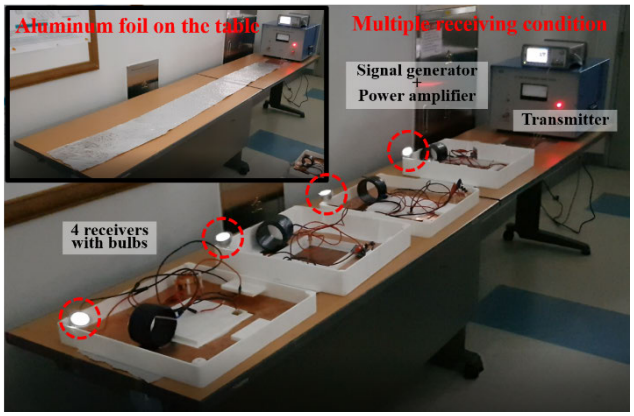

FIGURE 14. Test setup of the multiple-receiving MSG-WPT system with the four receiving parts using a 4 W bulb on 3.5 m of aluminum foil.

To quantitatively measure the change in received power from the LED bulb when the number of Rxs increases, one Tx is installed on a 3.5 m aluminum foil, and an Rx is installed at the other end, as shown in Fig. 14. When increasing the number of Rxs from 1 to 4, the voltage at both ends of the LED bulb of the first placed Rx is measured. The measurement results are presented in Fig. 15. The solid black line is the measured voltage across the LED bulb with one Tx and one Rx placed on the aluminum foil. In the case of the solid red line, the number of Rxs is increased to 4 in the same environment as the initial case, and the voltage at both ends of the LED bulb of the initially placed Rx is measured. As seen from the graph, there is little change in the magnitude of the voltage at the initially placed Rx by comparing the situation

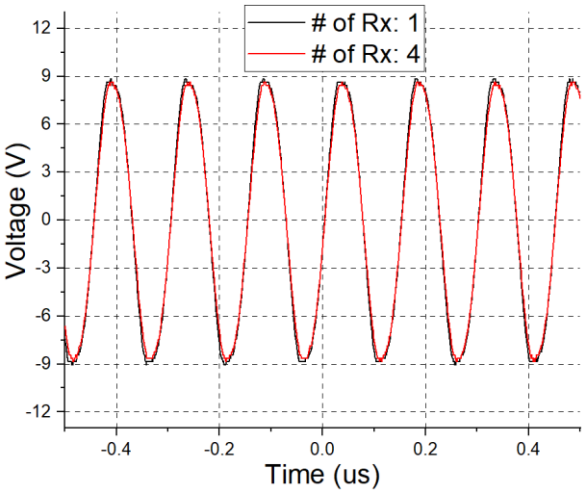

FIGURE 15. Measured voltage across the LED at the input of receiver #1: the receiver by itself and when four receivers are lit.

with between 1 Rx and 4 Rxs. Similar measurement results are obtained when the number of Rxs is 2 and 3; however, these results are not added to the graph to avoid complexity. The same voltage measurements are obtained from the LED bulbs of the other Rxs.

IV. CONCLUSION

With the necessity for wireless charging systems in the era of IoT, significant research with the radiative and nonradiative WPT has been reported, especially nonradiative WPT. However, there are two major issues with variations in the PTE of nonradiative WPT: the misalignment and distance between the Tx and Rx. Further research into advancing existing techniques or novel systems for WPT is necessary to resolve these challenges. Moreover, it is desirable for the WPT system to easily provide power to multiple Rxs with a single Tx.

In this paper, an MSG-WPT system with a CPE was proposed for portable wireless power receiving applications without any concerns of orientation or alignment between Tx and multiple Rxs. The PWPE was analyzed, and its tunable design parameters were deduced to enhance the PTE. Based on our analysis, the lumped inductor and capacitor substituted for the PWPE in the receiving part increased the portability of the system. The substitution was considered in the L-section lumped impedance-matching scheme from the derived equivalent circuit model. The CPE was employed in the L-section impedance-matching scheme, instead of the lumped inductor, to improve the received power intensity. We also presented the equivalent circuit model of the proposed system, considering all possible scenarios. The proposed MSG-WPT system can be utilized in applications with multiple receivers on regular aluminum foil. The prototype was developed, and the peak PTE was measured to be approximately -12 dB with resonance frequency at 4 MHz, proving that our system was a significant improvement over the existing systems.

ACKNOWLEDGMENT

(Woojin Park and Bonyoung Lee contributed equally to this work.)

REFERENCES

[1] H. Solar, M. Alonso, P. Bustamante, and C. Giers, "Design of a wireless power transfer receiver with an ad-hoc coil for the Qi standard," in *Proc. Conf. Design Circuits Integr. Syst. (DCIS)*, Nov. 2015, pp. 1–5.

[2] A. Kurs, A. Karalis, R. Moffatt, J. D. Joannopoulos, P. Fisher, and M. Soljacic, "Wireless power transfer via strongly coupled magnetic resonances," *Science*, vol. 317, no. 5834, pp. 83–86, Jul. 2007.

[3] J. Kim, H.-C. Son, K.-H. Kim, and Y.-J. Park, "Efficiency analysis of magnetic resonance wireless power transfer with intermediate resonant coil," *IEEE Antennas Wireless Propag. Lett.*, vol. 10, pp. 389–392, 2011.

[4] J. Jadidian and D. Katabi, "Magnetic MIMO: How to charge your phone in your pocket," in *Proc. 20th Annu. Int. Conf. Mobile Comput. Netw.*, Sep. 2014, pp. 495–506.

[5] B.-C. Park, J.-H. Kim, and J.-H. Lee, "Mode reconfigurable resonators insensitive to alignment for magnetic resonance wireless power transmission," *IEEE Microw. Wireless Compon. Lett.*, vol. 24, no. 1, pp. 59–61, Jan. 2014.

[6] Z. Dang, Y. Cao, and J. A. A. Qahouq, "Reconfigurable magnetic resonance-coupled wireless power transfer system," *IEEE Trans. Power Electron.*, vol. 30, no. 11, pp. 6057–6069, Apr. 2015.

[7] Z. Dang and J. A. A. Qahouq, "Extended-range two-coil adaptively reconfigurable wireless power transfer system," in *Proc. IEEE Appl. Power Electron. Conf. Expo. (APEC)*, Mar. 2015, pp. 1630–1636.

[8] Y. Cao, Z. Dang, J. A. A. Qahouq, and E. Phillips, "Dynamic efficiency tracking controller for reconfigurable four-coil wireless power transfer system," in *Proc. IEEE Appl. Power Electron. Conf. Expo. (APEC)*, Mar. 2016, pp. 3684–3689.

[9] F. Jolani, Y.-Q. Yu, and Z. Chen, "A planar magnetically-coupled resonant wireless power transfer using array of resonators for efficiency enhancement," in *IEEE MTT-S Int. Microw. Symp. Dig.*, May 2015, pp. 1–4.

[10] Z. Liu, Y. Guo, F. Jolani, Y. Yu, and Z. D. Chen, "Planar magnetically-coupled resonance wireless power transfer systems using array of coil resonators," in *IEEE MTT-S Int. Microw. Symp. Dig.*, Mar. 2016, pp. 1–3.

[11] Z. Liu, Z. Chen, Y. Guo, and Y. Yu, "A novel multi-coil magnetically-coupled resonance array for wireless power transfer system," in *Proc. IEEE Wireless Power Transf. Conf. (WPTC)*, May 2016, pp. 1–3.

[12] D. Ahn and S. Hong, "Effect of coupling between multiple transmitters or multiple receivers on wireless power transfer," *IEEE Trans. Ind. Electron.*, vol. 60, no. 7, pp. 2602–2613, Jul. 2013.

[13] H. Yin, M. Fu, C. Zhao, and C. Ma, "Power distribution of a multiple-receiver wireless power transfer system: A game theoretic approach," in *Proc. 41st Annu. Conf. IEEE Ind. Electron. Soc. (IECON)*, Nov. 2015, pp. 001776–001781.

[14] M. Fu, T. Zhang, C. Ma, and X. Zhu, "Efficiency and optimal loads analysis for multiple-receiver wireless power transfer systems," *IEEE Trans. Microw. Theory Techn.*, vol. 63, no. 3, pp. 801–812, Mar. 2015.

[15] Y. Zhang, T. Lu, Z. Zhao, F. He, K. Chen, and L. Yuan, "Selective wireless power transfer to multiple loads using receivers of different resonant frequencies," *IEEE Trans. Power Electron.*, vol. 30, no. 11, pp. 6001–6005, Nov. 2015.

[16] S. K. Oruganti, O. Kaiyrakhmet, and F. Bien, "Wireless power and data transfer system for Internet of Things over metal walls and metal shielded environments," in *Proc. URSI Asia–Pacific Radio Sci. Conf. (URSI AP-RASC)*, Aug. 2016, pp. 318–320.

[17] S. K. Oruganti, F. Liu, D. Paul, J. Liu, J. Malik, K. Feng, H. Kim, Y. Liang, T. Thundat, and F. Bien, "Experimental realization of Zenneck type wave-based non-radiative, non-coupled wireless power transmission," *Sci. Rep.*, vol. 10, no. 1, pp. 1–12, Dec. 2020.

[18] X. Ma, M. S. Mirmoosa, and S. A. Tretyakov, "Parallel-plate waveguides formed by penetrable metasurfaces," *IEEE Trans. Antennas Propag.*, vol. 68, no. 3, pp. 1773–1785, Mar. 2020.

FRANKLIN BIEN (Senior Member, IEEE) received the B.S. degree in electronics engineering from Yonsei University, Seoul, South Korea, in 1997, and the M.S. and Ph.D. degrees in electrical and computer engineering from the Georgia Institute of Technology, Atlanta, GA, USA, in 2000 and 2006, respectively.

He is currently a Full Professor with the School of Electrical and Computer Engineering, Ulsan National Institute of Science and Technology (UNIST), Ulsan, South Korea. Prior to joining UNIST, in 2009, he was a Senior IC Design Engineer with Staccato Communications, San Diego, CA, USA, working on analog/mixed-signal IC and RF front-end circuits for ultrawideband (UWB) products, such as wireless USB in 65-nm CMOS technologies. Prior to working at Staccato, he was with Agilent Technologies and Quellan Inc., developing transceiver ICs for enterprise segments that improve the speed and reach of communication channels in consumer, broadcast, enterprise, and computing markets. His current research interests include circuits for wireless power transfer technologies, analog/RF IC design for consumer electronics, vehicular electronics, and biomedical applications.

WOOJIN PARK (Graduate Student Member, IEEE) was born in Seoul, South Korea, in 1990. He received the B.S. degree in electrical engineering from Dankook University, Yongin, South Korea, in 2016. He is currently pursuing the combined M.S.-Ph.D. degree in electrical engineering with the Ulsan National Institute of Science and Technology (UNIST), Ulsan, South Korea. His current research interests include the system design of wireless power transfer technologies and the circuits of power management ICs for implantable biomedical applications.

BONYOUNG LEE (Graduate Student Member, IEEE) was born in Busan, Republic of Korea, in 1994. He received the B.S. degree in electrical engineering from the Ulsan National Institute of Science and Technology (UNIST), Ulsan, Republic of Korea, in 2016, where he is currently pursuing the combined M.S.-Ph.D. degree in electrical engineering. His main research activities are focused on wireless power transfer (WPT) and its related circuits along with microwave engineering research.

GANGIL BYUN (Member, IEEE) received the B.S. and M.S. degrees in electronic and electrical engineering from Hongik University, Seoul, South Korea, in 2010 and 2012, respectively, and the Ph.D. degree in electronics and computer engineering from Hanyang University, Seoul, in 2015.

After his graduation, he returned to Hongik University to work as a Research Professor and performed active research for two years. He joined the faculty of the Ulsan National Institute of Science and Technology (UNIST), in 2018, where he is currently an Assistant Professor of electrical and computer engineering. His principal areas of research are in the design and analysis of small antenna arrays for adaptive beamforming applications, such as the direction of arrival estimation, interference mitigation, and radar. His recent research interests include circularly polarized antennas, vehicular and aeronautic antennas, global positioning system antennas, and antenna and array configuration optimization. He has actively contributed to the consideration of both antenna characteristics and signal processing perspectives for the improvement of overall beamforming performances.